Eur. Phys. J. A **15**, 459–462 (2002)
DOI 10.1140/epja/i2002-10044-6

THE EUROPEAN PHYSICAL JOURNAL A

First identification of excited states in ^{59}Zn

C. Andreoiu[1,a], M. Axiotis[2], G. de Angelis[2], J. Ekman[1], C. Fahlander[1], E. Farnea[2], A. Gadea[2], T. Kröll[2,b], S.M. Lenzi[3], N. Mărginean[4,2], T. Martinez[2], M.N. Mineva[1], C. Rossi Alvarez[3], D. Rudolph[1], and C.A. Ur[3,4]

[1] Department of Physics, Lund University, S-22100 Lund, Sweden
[2] INFN, Laboratori Nazionali di Legnaro, I-35020 Legnaro, Italy
[3] Dipartamento di Fisica dell'Università and INFN, Sezione di Padova, I-35131 Padova, Italy
[4] National Institute for Physics and Nuclear Engineering-"Horia Hulubei", RO-76900, Bucharest, Romania

Received: 28 May 2002 / Revised version: 28 June 2002 /
Published online: 3 December 2002 –
Communicated by W. Henning

Abstract. Excited states in ^{59}Zn were observed for the first time following the fusion-evaporation reaction ^{24}Mg + ^{40}Ca at a beam energy of 60 MeV. The GASP array in conjunction with the ISIS Silicon ball and the NeutronRing allowed for the detection of γ-rays in coincidence with evaporated light particles. The mirror symmetry of ^{59}Zn and ^{59}Cu is discussed.

PACS. 21.60.Cs Shell model – 23.20.Lv Gamma transitions and level energies – 27.50.+e $59 \leq A \leq 89$

Due to the charge symmetry of the nuclear force, mirror nuclei present similar energy level structures. The Coulomb interaction is responsible for any small difference between energy levels of two nuclei at equal spins. In the $f_{7/2}$ shell, mirror nuclei were previously studied up to $A = 49$ [1].

Recently, excited states in the $A = 51$ mirror nuclei ^{51}Fe and ^{51}Mn were reported up to terminating states [2, 3]. A few excited states are known for the $A = 53$ [4], $A = 55$ [5], and $A = 57$ [6] mirror partners. The present study aims at excited states in the $T = 1/2$ mirror partners ^{59}Zn and ^{59}Cu, which may allow for a more precise test of Coulomb matrix elements in the upper fp shell. So far, only the $3/2^-$ ground state of ^{59}Zn has been observed in β-decay [7,8], while excited states in ^{59}Cu [9–11] are well known.

The heavy-ion fusion-evaporation reaction ^{24}Mg + ^{40}Ca at a beam energy of 60 MeV was used to populate excited states in $N \sim Z$ nuclei in the mass $A \approx 60$ region. A 4-particle nA ^{24}Mg beam was delivered by the Tandem XTU accelerator of Legnaro National Laboratory. The $A = 59$ mirrors ^{59}Zn and ^{59}Cu were produced via evaporation of one α-particle and one neutron and one α-particle and one proton, respectively. The γ-rays were detected with the GASP array [12] in its standard configuration with 40 HPGe detectors, coupled to the 4π charged-particle detector ISIS [13] composed of 40 ΔE-E Si telescopes, and the NeutronRing array replacing six of the 80 BGO elements at the most forward angles. The beam energy was close to the Coulomb barrier, and thus it was favourable for the evaporation of two particles from the ^{64}Ge compound system. In the 0.5 mg/cm^2 thick, enriched (nominally 99.98%) ^{40}Ca target layer the beam energy was reduced to some 55 MeV. At this energy no significant fusion cross-section is predicted any more. The target was backed by 7 mg/cm^2 tantalum to stop the recoils but to be as transparent as possible for evaporated charged particles. The α-particle efficiency estimated for the present experiment is $\epsilon_\alpha \sim 40(2)\%$, which is in accordance with ref. [13]. A relative cross-section of $\sigma_{\rm rel} \sim 0.02\%$ of the total fusion-evaporation cross-section for the $1\alpha1$n channel was estimated. Gamma-rays detected in coincidence with charged particles and neutrons provide reaction channel selection.

The identification of ^{59}Zn was first done by comparing the $1\alpha0$p1n- and $1\alpha1$p1n-gated spectra. The transitions present only in the $1\alpha0$p1n-gated spectrum are good candidates for ^{59}Zn, while transitions present in both spectra can be disregarded. Figure 1(a) shows two spectra in coincidence with $1\alpha0$p1n (black line) and $1\alpha1$p1n (grey line). There is an enhancement of counts at 894 keV in the $1\alpha0$p1n spectrum with respect to the $1\alpha1$p1n spectrum. The energy is similar to the most intense transition in ^{59}Cu at 914 keV, and the peak at 894 keV is suggested to be the $(5/2^-) \rightarrow 3/2^-$ transition in ^{59}Zn.

It is important to check this assignment against transitions with similar energies from known contaminating

[a] *Present address:* Oliver Lodge Laboratory, University of Liverpool, P.O. Box 147, Liverpool, L69 7ZE, United Kingdom; e-mail: ca@ns.ph.liv.ac.uk.
[b] *Present address:* Physik-Departament, Technische Universität München, D-85748 Garching, Germany.

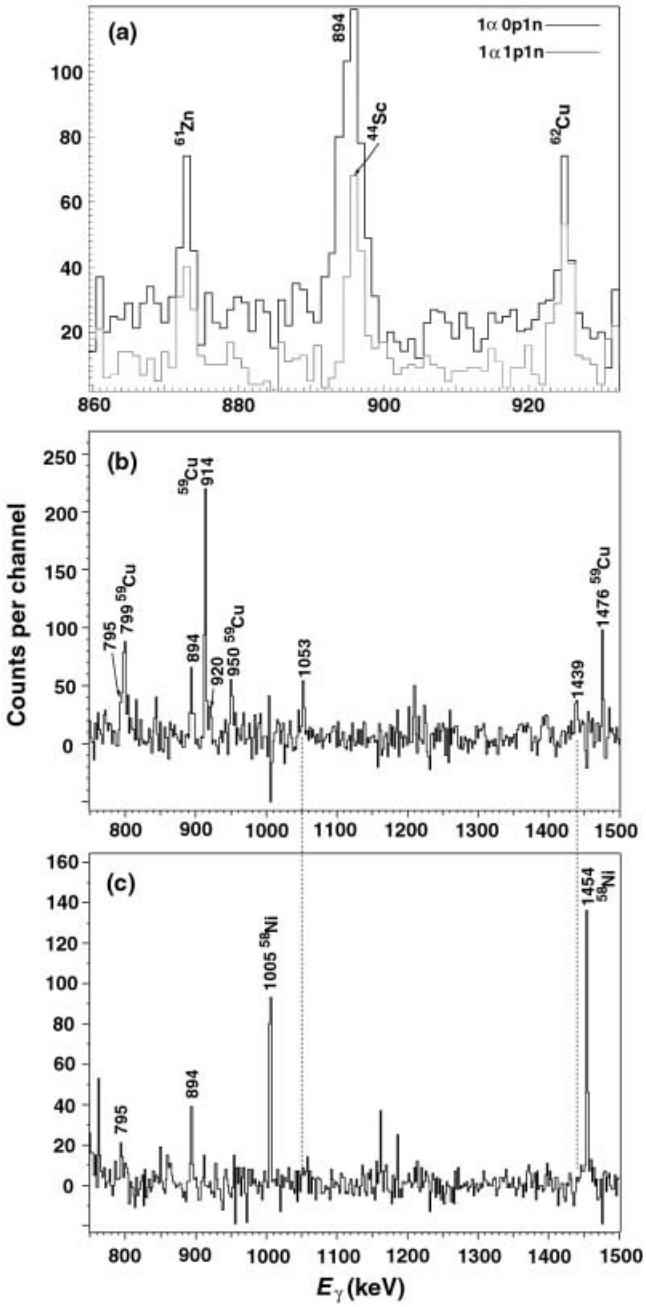

Fig. 1. (a) Gamma-ray spectra in coincidence with one α-particle, zero protons, and one neutron (1α0p1n, black line) and one α-particle, one proton, and one neutron (1α1p1n, grey line). The transition at 894 keV in the 1α0p1n-gated spectrum represents a good candidate for a ground-state transition in ^{59}Zn. (b) 1α0p-gated spectrum in coincidence with the 894, 1439, and 1053 keV transitions. (c) 1α0p-gated spectrum in coincidence with the 920 keV transition. See text for more details.

reaction channels by using available nuclear data evaluations [14]. The target contaminants in our experiment were small amounts of ^{12}C, ^{16}O, ^{44}Ca, and $^{\rm nat}$Mg. The latter is unusual and certainly larger than the number ($< 0.01\%$) provided by the vendor of the enriched ^{40}Ca target material. One possible explanation for the presence of some 1% $^{\rm nat}$Mg in the target is its acquisition during chemical processing in the course of the target production, because Mg and Ca belong to the same chemical group. As a result of the search two transitions near 894 keV have to be considered: the 893.8 keV $5^+ \rightarrow 7^+$ transition in ^{42}Sc and the 895.5 keV $(11)^+ \rightarrow (9)^+$ transition in ^{44}Sc, which may result from the ^{24}Mg(^{24}Mg, αpn)^{42}Sc and ^{26}Mg(^{24}Mg, αpn)^{44}Sc reactions, respectively. The 895.5 keV transition is in coincidence with transitions at, *e.g.*, 697 and 1703 keV and it is present in both spectra of fig. 1(a). This confirms its assignment to ^{44}Sc and is consistent with the production in a 1α1p1n reaction channel. On the contrary, the 893.8 keV transition is absent in the 1α1p1n-gated spectrum of fig. 1(a). Moreover, the initial state of the 893.8 keV transition in ^{42}Sc belongs to a non-yrast structure, which are at most weakly populated in heavy-ion–induced fusion-evaporation reactions. The other two transitions in the spectra of fig. 1(a) belong to intense yrast transitions in ^{61}Zn (872 keV; $7/2^- \rightarrow 5/2^-$) [15] and ^{62}Cu (925 keV; $6^- \rightarrow 5^+$) [16], respectively. Transitions from ^{61}Zn, which marks the strongest reaction channel involving neutron evaporation in our experiment, leak weakly into the spectra of fig. 1(a) due to imperfect proton-α discrimination and/or pile-up events in the detector elements of ISIS. Transitions from ^{62}Cu originate from the ^{44}Ca(^{24}Mg, αpn)^{62}Cu reaction. Even though the evaporation of neutrons is much more likely following reactions on ^{44}Ca than on ^{40}Ca, the yield of transitions from ^{62}Cu hints at a somewhat larger ^{44}Ca impurity than given by the vendor of the enriched ^{40}Ca target material ($< 0.02\%$). Possible yrast transitions from ^{63}Zn [17], which corresponds to the 1α0p1n reaction channel of the ^{24}Mg + ^{44}Ca reaction, are different from those assigned to ^{59}Zn and not visible in the spectrum of fig. 1(a).

The analysis of $\gamma\gamma$ spectra gated with one α-particle, zero protons and one neutron, 1α0p1n, was not possible because of lack of statistics. Therefore, the neutron coincidence was relaxed, and 1α0p-gated spectra were used for the $\gamma\gamma$ analysis. After the identification of the first candidate at 894 keV, two more transitions at 1439 and 1053 keV were observed in a 1α0p-gated γ-ray spectrum in coincidence with the 894 keV line. Figure 1(b) presents the 1α0p-gated γ-ray spectrum in coincidence with the 894, 1053, and 1439 keV transitions. It shows the transitions at 894, 1053, and 1439 keV, and two more transitions at 795 and 920 keV, which also are suggested to belong to ^{59}Zn. Because the proton escaped detection, a few transitions at 799, 914, 950, and 1476 keV belonging to the 1α1p channel ^{59}Cu are present in the 1α0p spectrum in fig. 1(b).

Ratios of intensities of γ-ray transitions in coincidence with 1α0p and 0α0p are plotted in fig. 2. They confirm the assignment of the above-mentioned γ-rays to ^{59}Zn. The intensities of γ transitions of known exit channels were obtained from spectra gated on intense transitions in the respective nucleus. The reference points are from transitions in ^{56}Ni (2α channel, squares), and transitions in ^{59}Cu (1α1p channel, diamonds). For comparison, the intensity ratios deduced from detection probabilities calculated ac-

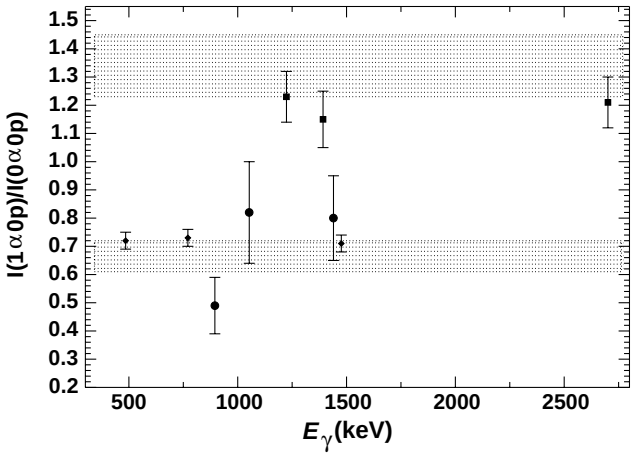

Fig. 2. Intensity ratios for selected γ-rays obtained from 1α0p- and 0α0p-gated spectra *versus* γ-ray energy for different exit channels. See text for more details.

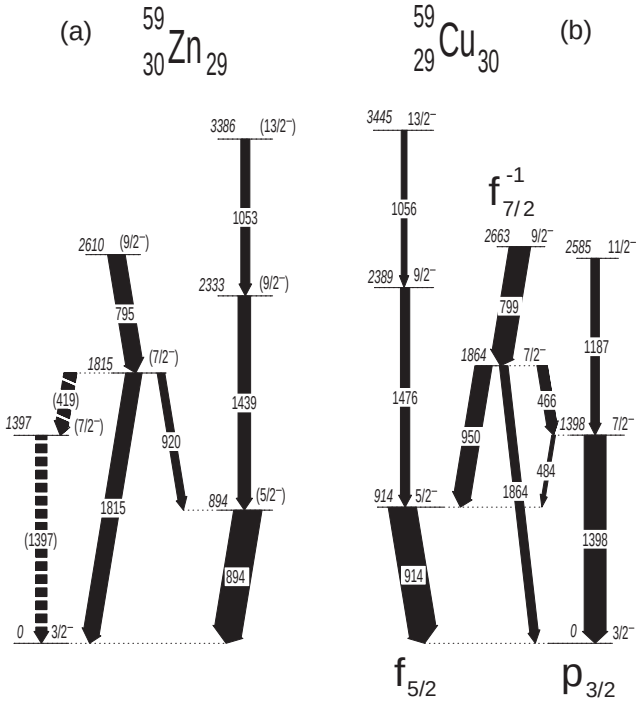

Fig. 3. Partial decay schemes of the $A = 59$ ^{59}Zn (obtained from the present analysis) and ^{59}Cu [9–11] mirror nuclei. The widths of the arrows of the transitions are proportional to their relative intensities and the energy labels are in keV. Based on the mirror symmetry, spins and parities of states in ^{59}Zn are assigned tentatively.

cording to ref. [18] with an α detection efficiency of $\varepsilon_\alpha \sim 40(2)\%$ are marked by the dotted areas in fig. 2. The circles represent the transitions at 894, 1439, and 1053 keV. They are lying in the region corresponding to an exit channel involving the evaporation of one α-particle. The spectra in fig. 1(a) and (b) demonstrate that the 894, 1439, and 1053 keV transitions belong to a 0p1n channel. Reaction channels involving the evaporation of one α-particle and

Table 1. Excitation energies, γ-ray energies, relative intensities, suggested spin and parities assigned to ^{59}Zn from the present experiment. The intensities are normalized to the 894 keV transition.

E_x (keV)	E_γ (keV)	$I_{\rm rel}$ (%)	$I_{\rm i}^\pi(\hbar)$	$I_{\rm f}^\pi(\hbar)$
894(1)	894(1)	100(15)	$(5/2^-)$	$3/2^-$
1397(2)	1397(2)	41(20)	$(7/2^-)$	$3/2^-$
1815(2)	419(1)	45(30)	$(7/2^-)$	$(7/2^-)$
	920(1)	27(11)	$(7/2^-)$	$(5/2^-)$
	1815(2)	58(26)	$(7/2^-)$	$3/2^-$
2333(2)	1439(2)	46(19)	$(9/2^-)$	$(5/2^-)$
2610(2)	795(1)	62(19)	$(9/2^-)$	$(7/2^-)$
3386(2)	1053(1)	33(16)	$(13/2^-)$	$(9/2^-)$

two or more neutrons are too weak in cross-section to be observed in the present experiment. The yrast bands in the ^{31}S [19] ^{35}Ar [19], ^{43,45}Ti [20,21] nuclei, which are produced in reactions with the target contaminants, are known [14]. Since coincidences between any combination of the 894, 1439, and 1053 keV lines do not occur in any other nuclei with $30 < A < 60$ the conclusion is that the 894, 1439, and 1053 keV cascade belongs to the 1α0p1n channel leading to ^{59}Zn.

The construction of the ^{59}Zn level scheme, which is presented in fig. 3(a), is based on the $\gamma\gamma$ coincidence analysis in the 1α0p-gated matrix. The intensities of the transitions are normalized to the 894 keV line, and they are summarized in table 1. Tentatively assigned spins and parities of the levels in ^{59}Zn are based on the mirror symmetry with ^{59}Cu and thus are given in brackets. We have assigned the 1439 keV line to the $(9/2^-) \rightarrow (5/2^-)$ transition, and the 1053 keV line to the $(13/2^-) \rightarrow (9/2^-)$ transition. A 1α0p γ-ray spectrum in coincidence with the 1053 keV line confirms the coincidence with the 894 and 1439 keV transitions, but not with the 795 and 920 keV lines. Figure 1(c) shows a 1α0p γ-ray spectrum in coincidence with the 920 keV transition. This line is obviously in coincidence with the transitions at 894 and 795 keV, but not with the 1439 and 1053 keV lines. Consequently, the 920 keV line was placed on a parallel branch with the 1439 keV line, depopulating the 1815 keV $(7/2^-)$ level. On top, the 795 keV $(9/2^-) \rightarrow (7/2^-)$ transition was added. We have also observed a transition at 1815 keV in coincidence with the 795 keV transition, which depopulates the 1815 keV level and matches the sum of the 920 and 894 keV lines. Parallel with this, we place two tentative transitions at 419 and 1397 keV, which may depopulate the 1815 keV level. Their sum also matches 1815 keV, and they have a pattern similar to the 466 and 1398 keV transitions in ^{59}Cu in fig. 3(b).

In fig. 4 the differences in level energies, the so-called Coulomb Energy Differences (CED), between ^{59}Zn and ^{59}Cu are plotted as a function of angular momentum. According to a simple shell-model picture for the low-spin states in ^{59}Cu [9,11], the 2585 keV $11/2^-$, the 1398 keV $7/2^-$ and the $3/2^-$ ground states can be generated by coupling a proton in the $p_{3/2}$ orbital to two neutrons in any of

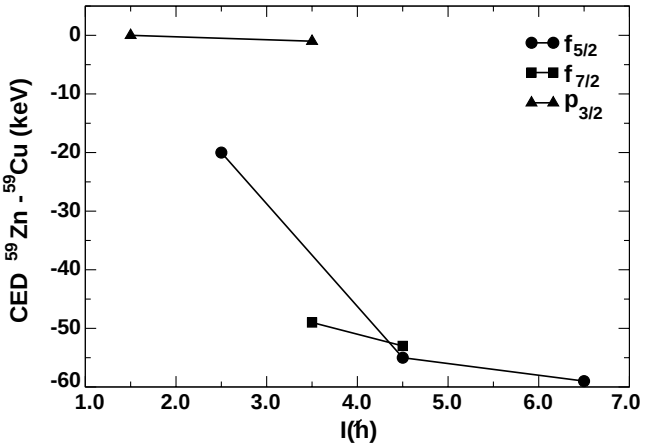

Fig. 4. Coulomb Energy Difference (CED) diagram for the $A = 59$ ^{59}Cu and ^{59}Zn mirror nuclei as a function of angular momentum. The triangles correspond to the $3/2^-$ ground-state band, the squares represent the second $7/2^-$ and $9/2^-$ states, and the circles show the $5/2^-$, $9/2^-$ and $13/2^-$ sequence.

the upper fp shell orbitals, *i.e.*, $\pi(p_{3/2})\otimes\nu(fp)^2_{0,2,4}$ (triangles in fig. 4). Similarly, the sequence of states at 914 keV $5/2^-$, 2389 keV $9/2^-$, and 3445 keV $13/2^-$ are interpreted as $\pi(f_{5/2})\otimes\nu(fp)^2_{0,2,4}$ (circles). The 1864 keV $7/2^-$ and 2663 keV $9/2^-$ states in ^{59}Cu (squares) are based on the one-$1f_{7/2}$-hole configuration $\pi(f_{7/2})^{-1}\pi(fp)^2_{0,2,4}\otimes\nu(fp)^2_{0,2,4}$. In ^{59}Cu this configuration was observed up to the fully aligned $23/2^-$ state.

A decrease of the CED with angular momentum is a consequence of breaking and aligning proton and neutron pairs in ^{59}Zn and ^{59}Cu, respectively. The average distance between protons increases, thus reducing the repulsive Coulomb force. This is reflected in the negative CED values. Compared to other CED values in mirror nuclei in the fp shell, the CED values for the $A = 59$ pair are relatively small. One explanation might be that by simple shell-model calculations the low-spin states in ^{59}Cu are mixed [11], and thus the Coulomb effects are quenched.

According to ref. [11], the wave functions are dominated by these intuitively derived configurations, but they are strongly mixed. For example, the $3/2^-$ ground state in ^{59}Cu contains only a 30% $\pi(p_{3/2})\otimes\nu(fp)^2_0$ closed core partition, while the $5/2^-$ state at 914 keV comprises only 20% of the $\pi(f_{5/2})\otimes\nu(fp)^2_0$ configuration.

In summary, we have established a level scheme of the ^{59}Zn nucleus for the first time. The scheme is similar to the level scheme of the mirror partner of ^{59}Cu. Coulomb effects present a typical behaviour, but they are smaller than in other mirror nuclei in the fp shell.

We would like to thank the accelerator crew at LNL for the excellent support. This research was supported by the Swedish Research Council and the European Commission under contract number HPRI-1999-CT-00083. C.A. acknowledges the support from the Gunnar and Gunnel Källen foundation and the kind hospitality at LNL.

References

1. M.A. Bentley *et al.*, in *Proceedings of the International Workshop Pingst 2000 - Selected Topics on N = Z Nuclei, June 2000, Lund, Sweden*, edited by D. Rudolph, M. Hellström (Bloms i Lund AB, 2000) p. 222.
2. J. Ekman *et al.*, Eur. Phys. J. A **9**, 13 (2000).
3. M.A. Bentley *et al.*, Phys. Rev. C **62**, 051303(R) (2000).
4. H. Junde, Nucl. Data Sheets **87**, 507 (1999).
5. D. Rudolph *et al.*, Z. Phys. A **358**, 379 (1997).
6. X.G. Zhou *et al.*, Phys. Rev. C **53**, 982 (1996).
7. J. Honkanen *et al.*, Nucl. Phys. A **366**, 109 (1981).
8. Y. Arai *et al.*, Nucl. Phys. A **420**, 193 (1984).
9. S. Juutinen, J. Hattula, M. Jääskeläinen, A. Virtanen, T. Lönnroth, Nucl. Phys. A **504**, 205 (1989).
10. C. Andreoiu *et al.*, Phys. Rev. C **62**, 051301(R) (2000).
11. C. Andreoiu *et al.*, Eur. Phys. J. A **14**, 317 (2002).
12. C. Rossi Alvarez, Nucl. Phys. News, Vol. **3**, 3 (1993).
13. E. Farnea *et al.*, Nucl. Instrum. Methods Phys. Res. A **400**, 87 (1997).
14. `http://www.nndc.bnl.gov/`; `http://radware.phy.ornl.gov/`.
15. M.R. Bhat, Nucl. Data Sheets **88**, 417 (1999).
16. B. Mukherjee *et al.*, Phys. Rev. C **63**, 057302 (2001).
17. B. Erjun, H. Junde, Nucl. Data Sheets **92**, 147 (2001).
18. S.Y. Van der Werf, Nucl. Instrum. Methods **153**, 221 (1978).
19. P.M. Endt, Nucl. Phys. A **521**, 1 (1990).
20. J.A. Cameron, B. Singh, Nucl. Data Sheets **92**, 783 (2001).
21. T.W. Burrows, Nucl. Data Sheets **65**, 1 (1992).